Sensors & Transducers, Vol. 259, Issue 5, October 2022, pp. 82-92

www.sensorsportal.com

Sensors & Transducers

Published by IFSA Publishing, S. L., 2022
http://www.sensorsportal.com

Low-cost Integrated Photonic Platform Developed via a Sol-gel Dip-coating Method: A Brief Review

[1] Łukasz KOZŁOWSKI, [1] Muhammad SHAHBAZ, [1, *] Muhammad Ali BUTT, [2] Cuma TYSZKIEWICZ, [2] Paweł KARASIŃSKI, [1] Andrzej KAŹMIERCZAK and [1] Ryszard PIRAMIDOWICZ

[1] Warsaw University of Technology, Institute of Microelectronics and Optoelectronics, Koszykowa 75, 00-662 Warszawa, Poland
[2] Silesian University of Technology, Department of Optoelectronics, ul. B. Krzywoustego 2, 44-100 Gliwice, Poland
E-mail: ali.butt@pw.edu.pl

Received: 31 August 2022 /Accepted: 3 October 2022 /Published: 31 October 2022

Abstract: Optical devices and circuits are now key elements in a variety of applications, including biotechnology, automotive, food quality control, chemistry, etc. It is highly desired to find low-cost solutions to the photonics integrated circuits (PICs). In this paper, a comprehensive review of silica-titania (SiO_2:TiO_2) materials obtained by a sol-gel method come together with a dip-coating technique, and the numerical analysis of different optical devices based on the SiO_2:TiO_2 optical platform are discussed. The sol-gel method is highly effective and does not require the use of expensive high-tech equipment. We discuss recent progress in our consortium on a cost-effective SiO_2:TiO_2 optical platform for integrated photonics applications, with a concentration on materials, devices, and optical sensing principles investigated via numerical simulations.

Keywords: Integrated photonics, Photonic integrated chip, Photonic sensor, Ring resonator, Grating, Photonic crystal, Silica titania, Sol-gel dip-coating method.

1. Introduction

Optical devices and circuits are now essential components in various applications, including biotechnology, automotive, food quality control, and chemistry, to mention a few. The attraction in optical sensing is supported by the exceptional benefits made possible by photonic technologies, such as high sensitivity, low cost, compactness, integration with electronic devices, and metal-free operation. Since technology has advanced so quickly in the last decade, silicon (Si) photonics has become one of the most efficient technology platforms for producing a wide range of functional optical components [1-5].

On the other hand, silica (SiO_2), titania (TiO_2), and silica-titania (SiO_2:TiO_2) materials obtained by the sol-gel technique have received much attention due to their potential optical applications [6-9]. The substantial performance of integrated photonic sensors is supported by technological characteristics and advances, among which ring resonators, subwavelength gratings (SWG), and one-dimensional photonic crystals (PhC) have fascinated the attention of scientists in recent years [6, 10-12]. In the following

sections, we discuss the recent developments on a low-cost silica-titania optical platform for integrated photonics applications, with special consideration to materials, devices, and optical sensing principles based on the numerical analysis performed in our group. Building planar (1D) and ridge (2D) waveguides for photonic integrated circuits (PICs) with acceptable optical characteristics and low optical transmission losses has been processed using SiO_2, TiO_2, and SiO_2:TiO_2 compounds obtained by the sol-gel method [13-15]. The sol-gel method and dip-coating technique are simple and inexpensive [16]. They allow the coating of large surfaces and do not require extremely high-temperature processing. Fabrication of high-quality thin films with exceptional thermal and mechanical stability using them is possible [17, 18]. A sufficient refractive index (R.I) contrast (Δn) between the substrate and the guiding layer is required for a functional WG [19].

The refractive indices and thickness of sol-gel films can be modified by fine-tuning the set-off precursors and solvents, in addition to the compound molar ratio and reaction temperature. Rare-earth elements [20, 21], laser dyes [22], and other organic compounds [23] can be doped into these WGs, permitting SiO_2 and TiO_2 sol-gel materials to be utilized in optical amplifiers, laser-active media, and sensing applications [24, 25]. The sol-gel process is highly effective and does not necessitate using pricey high-tech equipment. The sol-gel technique can adjust the R.I of the waveguide films. The optical losses sustained by these waveguides are equivalent to waveguides obtained using the chemical vapor deposition (CVD)/low-pressure chemical vapor deposition (LPCVD) method [26, 27]. Several research groups have developed optical waveguides based on a silica-titanium platform for different applications in recent years [28-30].

A recent study [9] demonstrated a desirable waveguide platform based on SiO_2:TiO_2 that is simple to develop and inexpensive. The material is an excellent choice for the visible and near-IR wavelength range due to its broad transparency range. Another study [10] discussed developing an optical waveguide system utilizing the sol-gel method and dip-coating technique. The optical characterization of the waveguide system is investigated at a visible wavelength. However, the system can operate from visible to near-IR wavelength ranges.

The same approach involving the sol-gel method [11] is used to develop high-quality SiO_2:TiO_2 thin films on a glass substrate. The coating process produces thin films with reduced surface roughness and losses, making them an excellent choice for the waveguiding purpose. A recent work [6] proposes numerical modeling of extremely attractive SWG waveguides for filtering and sensing applications using the finite element method for modelling and nano-imprint lithography (NIL) process to develop low-cost integrated photonic devices. The experimental analyses of these sensor designs are yet to be performed. However, the development of the silica-titania platform and its characterization has been performed at the Silesian University of Technology, Poland.

2. Materials and Fabrication Process

The coating process involves depositing a thin layer of materials onto a substrate in either the solid or liquid phase (solution). According to production needs for coated layer thickness, coated surface roughness, rate, and coating product size—which can be determined by coating velocity, coated film width, and designing capabilities—coating strategies may be used. Silica titania (SiO_2: TiO_2) has been widely researched because of its potential optical properties and applications [31]. It is a material that constitutes the new low-cost technological platform for PICs via the aforementioned combination of the sol-gel method and dip-coating technique [32]. SiO_2:TiO_2 itself is a very attractive material regarding integrated photonics because its R.I may vary between 1.6-2.2 and its spectral range stands from visible to NIR [12]. Moreover, the material combined with this fabrication technique gives the possibility to create optical interconnects with minimal transmission losses [33-36].

First of all, the fabrication process of a single SiO_2:TiO_2 waveguide film will be discussed. This process is relatively simple [25, 37] as depicted in Fig. 1.

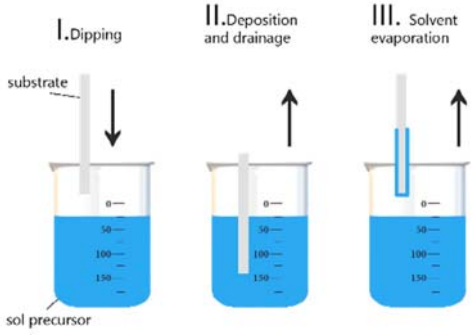

Fig. 1. Sol-gel dip-coating fabrication method.

To carry out the fabrication process the following components are required:

1. Substrate – which is the material on which SiO_2:TiO_2 will be deposited will be fully covered by it, creating a full SiO_2:TiO_2 waveguide film, e.g., soda-lime glass or BK7 glass. BK7 glass is preferred due to its lower thermal expansion coefficient and lower surface roughness.
2. Sol precursor – a previously prepared colloidal solution that contains the covering material, e.g., SiO_2:TiO_2.

The preparation of the sol precursor for SiO_2:TiO_2 consists of adding SiO_2 and TiO_2 precursors

respectively being tetraethyl ortosilicate (TEOS) and tetraethyl ortotitanate (TET) with a homogenizing factor which in this case was ethyl alcohol (C_2H_5OH). Further to carry out the reaction of hydrolysis and condensation, hydrochloric acid (HCl) needs to be used [13].

After having the BK7 glass covered by SiO_2:TiO_2 to harden the material it is necessary to carry out heat treatment. Numerous factors, such as pH and solution concentration, might have a significant impact on the efficacy of the dip-coating process by altering, for instance, its viscosity. Nevertheless, because coating techniques used in modern studies have been well-documented in earlier works, pH and solution viscosity are rarely discussed by writers. Using more viscous solutions causes more clumping and thicker coating layers, so fewer dip-coating cycles are necessary to achieve a specific thickness or amount of deposited mass. The resulting coating, meanwhile, may shatter and agglomerate particles in unfavorable locations. To get around these problems, the dip-coating technique might offer a more homogeneous coating by combining a less viscous solution with numerous repetitions.

As for the dependence of R.I on the variables of the process, it should be noted that it depends on the stoichiometric ratio between precursor components as shown in Fig. 2.

The withdrawal speed of the substrate from the sol affects predominately the thickness of the deposited film as presented in Fig. 3.

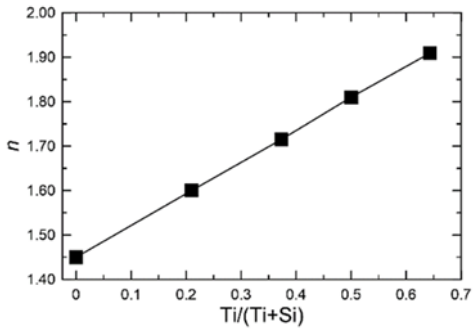

Fig. 2. Sol-gel dip-coating fabrication method [10].

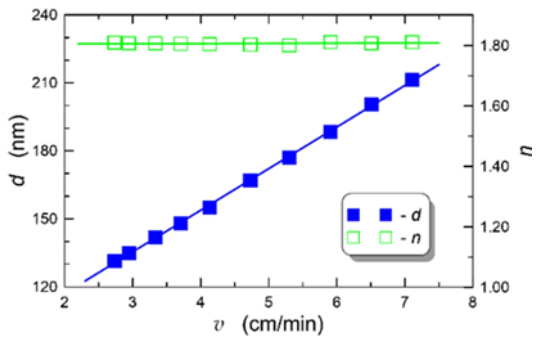

Fig. 3. Sol-gel dip-coating fabrication method [10].

The main benefit of using this method over other conventional methods of thin film deposition as plasma-enhanced chemical vapor deposition (PECVD), low-pressure chemical vapor deposition (LPCVD), or physical vapor deposition (PVD) is that it is much easier to conduct, extremely cheaper and does not require foundries or advanced equipment and laboratories [38].

Once the platform is prepared, the next step is the fabrication of waveguide interconnects and other waveguide structures. There are several methods of fabrication of such structures. Some approaches are shown in Fig. 4. All the following three methods are currently being explored in our consortium.

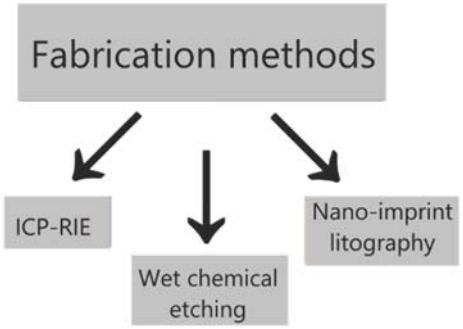

Fig. 4. WG structure fabrication processes.

An exemplary rib WG fabrication process via reactive ion etching (RIE) [39] is shown in Fig. 5.

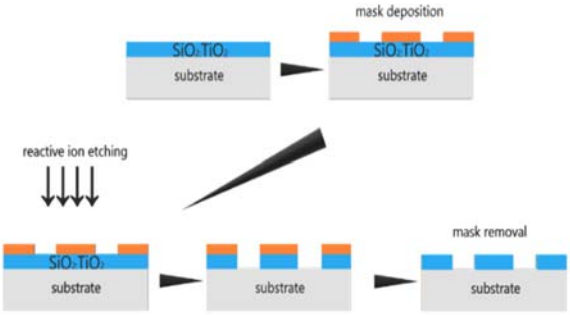

Fig. 5. SiO_2:TiO_2 ridge WG fabrication on a glass substrate.

The main design variables of a basic WG are its width w and its height h. Nevertheless, the crucial parameters for a WG to operate properly are the refractive indices of the WG, substrate, and ambient medium. In Fig. 4 the refractive indices are $n_{wg}=1.7$, $n_{sub}=1.5$, and $n_{amb}=1$.

Another interesting WG fabrication process [40] is shown in Fig. 6 which involves the wet-chemical etching of substrate and later on depositing a thin-film of SiO_2:TiO_2 material via the dip-coating method. This

WG structure can provide a low-cost solution to the PICs.

Both WGs shown in Fig. 5 and Fig. 6 are layouts that can be fabricated on SiO_2:TiO_2 with the use of the previously mentioned fabrication method.

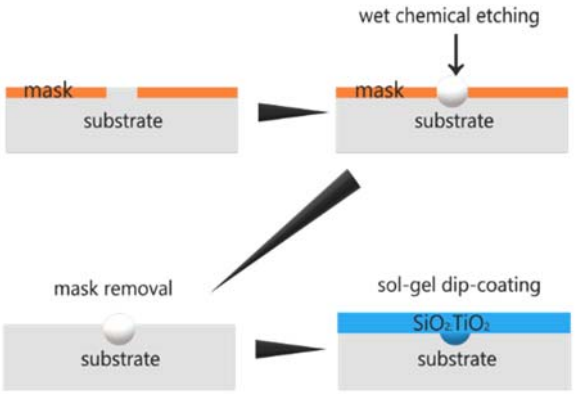

Fig. 6. Inverted rib waveguide fabrication on a glass substrate.

The most convenient method of fabricating waveguide interconnects and structures consist of lithography and etching. The mainstream technologies are electron beam lithography (EBL) or conventional UV lithography combined with RIE or inductively coupled plasma (ICP) RIE.

Those technologies are well-researched and applied for a long time which gives them the advantage of being reliable. However, those are technologies that require advanced and expensive laboratory equipment making them inaccessible and not cost-effective. To fabricate an integrated photonic chip, it is necessary to use the services of foundries.

The approach of using different methods that are not as expensive and do not require sophisticated equipment could be a game changer regarding integrated photonics. One of the technologies that could open a lot of new fabrication possibilities for integrated photonics could be nano-imprint lithography (NIL). The simplicity and cost-effectiveness of NIL are its biggest advantages over the previously mentioned conventional methods [11]. Nevertheless, this technology is not as well developed and well researched concerning other methods so it needs more time and attention to match other more well-known technologies.

The simplicity of NIL lies in the fact that it is easily reproducible and the fabrication of waveguide structures is etch-less. However, there are several variables such as force applied during imprinting, amount of sol-gel, and post-annealing temperature that should be properly optimized to avoid cracks and guarantee reproducibility. It is shown in Fig. 7. If some automatization would be added to the process, then it could revolutionize the whole integrated photonics industry.

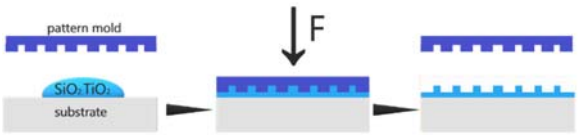

Fig. 7. NIL process.

3. Devices and Applications

The main and most interesting applications for PIC platforms based on SiO_2:TiO_2 materials would be sensing and biosensing. Of course, it can find many other functions same as other conventional materials used for integrated photonics [26, 41].

Three investigated structures for sensing involving: ring resonators, subwavelength gratings (SWG), and 1-D photonic crystals (1-D PhC) are discussed below.

3.1. Ring Resonators

The SiO_2:TiO_2 optical waveguide's R.I sensing capabilities were investigated using the ring resonator device [10]. Sensitivity (*S*), a figure of merit (*FOM*), and the *Q-factor* are three crucial factors that should be wisely considered while creating sensing devices. The following expression is used to determine the sensitivity of the ring resonator.

$$S = \frac{\Delta\lambda_{res}}{\Delta n}, \quad (1)$$

where $\Delta\lambda_{res}$ is the change in resonance wavelength and Δn represents the shift in ambient R.I.

The fraction of the sensitivity and full width at half maximum (FWHM) of the resonance dip is known as a *FOM*. *FOM* is calculated by using the following expression:

$$FOM = \frac{S}{FWHM} \quad (2)$$

For a variety of functions, integrated resonators with superior Q-factors are mostly needed. The Q-factor is calculated as follows:

$$Q - Factor = \frac{\lambda_{res}}{FWHM} \quad (3)$$

The ring resonators are particularly sensitive to changes in the ambient medium, resulting in the redshift of the resonance wavelength. The value of shift in the resonance wavelength depends on the device's geometric variables [10]. A schematic diagram of a ring resonator based on a SiO_2:TiO_2 optical waveguide is shown in Fig. 8.

The radius of the ring (*R*) was selected to be 15 μm. The distance of coupling between the bus waveguide and ring is symbolized as *g*. The surrounding medium

was filled with a dielectric material with an R.I of 1.33. The height of the device was set at 200 nm [10].

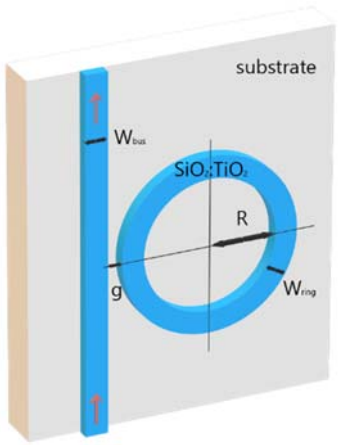

Fig. 8. A schematic view of a ring resonator based on SiO_2:TiO_2 optical waveguide [10].

3.1.1. Geometric Variables of the Ring Structure

Fig. 9a shows the ring resonator's transmission spectrum. It is worth mentioning that six resonance dips (λ_{dip}) with an FSR of ~6.4 nm and the FWHM of λ_{dip} ~0.44 nm were achieved, as illustrated in Fig. 9b. The coupling efficiency (CE) was calculated for each λ_{dip}, as illustrated in Fig. 9c. CE was calculated by estimating the ER of the bus waveguide and obtaining the ER for g in the 50-350 nm range. The max. value ER of ~2.5-2.6 dB was achieved for g = 250 nm to 300 nm [10].

3.1.2. Sensing Analysis and Device Performance

The R.I of the ambient medium was varied from 1.33 to 1.365 with 0.005 step size to test the sensing abilities of the sensor [10].

As the R.I of the ambient medium increased, the λ_{dip} executed a redshift, as shown in Fig. 10a. For this analysis, W_{bus} = W_{ring} = 800 nm was used, which resulted in substantial light confinement in the ring structure and a low evanescent field. As a result, light-matter interaction is low, with S = ~90 nm/RIU, FOM = ~204.5 RIU1, and Q-factor = 2239. Fig. 10b and Fig. 10c shows normalized electric field distributions at λ = 985.3 nm and = 987 nm, which correspond to the on-resonance and off-resonance states, respectively [10].

As we know, boosting the evanescent field ratio (EFR) can improve sensitivity. It is possible to get higher EFR by shrinking the width of the ring waveguide (W_{ring}). Reducing W_{ring} = 500 nm improved the *S*, *FOM*, and *Q-factor* of the device, as shown in Fig. 11.

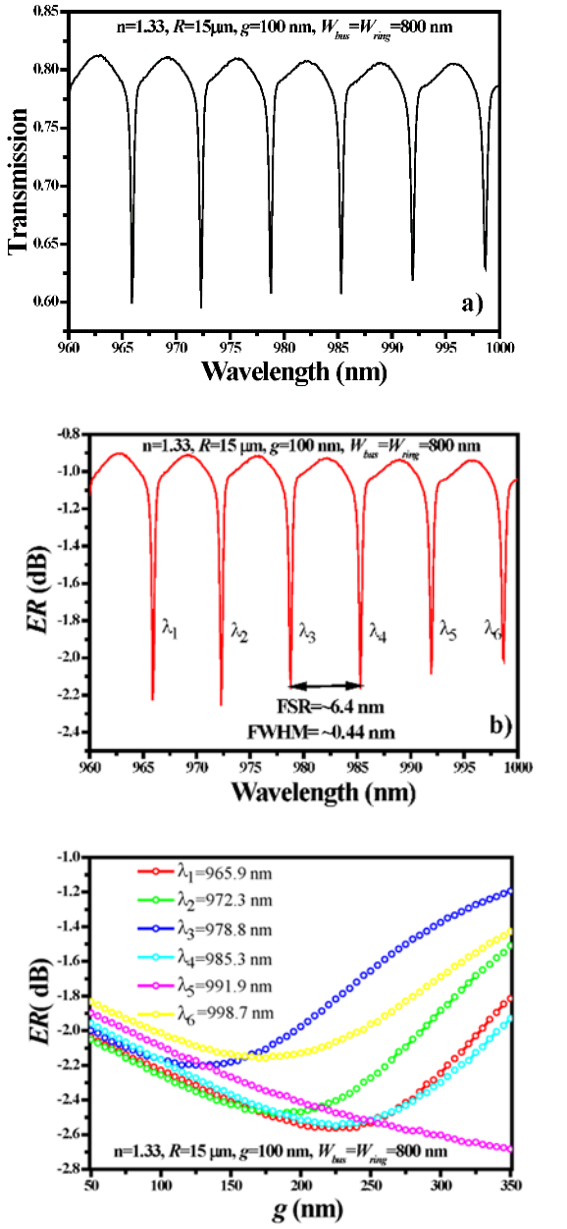

Fig. 9. Spectral properties of the ring resonator configuration: (a) transmission spectrum, (b) FSR vs ER, (c) optimization of g [10].

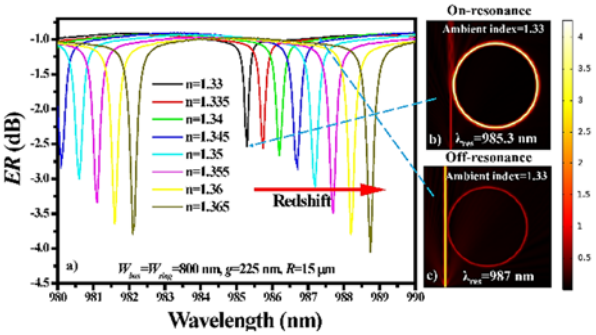

Fig. 10. (a) Transmission spectrum of the ring resonator with various ambient refractive indices. Distribution of norm. The electric field in the ring resonator structure in the (b) on-resonance state and (c) off-resonance state [10].

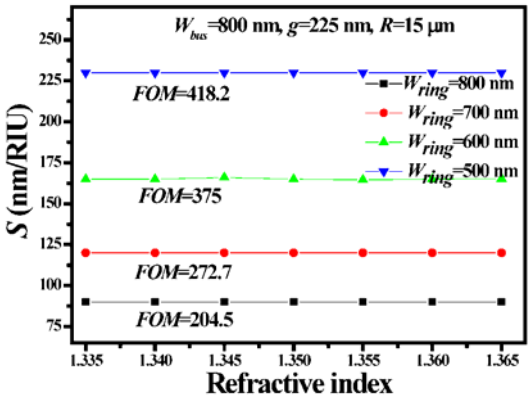

Fig. 11. Analysis of *S* and *FOM* depending on W_{ring}. The other geometric variables for instance W_{bus}, R , and g were set at 800 nm, 15 μm, and 225 nm, respectively [10].

3.1.3. Summary of the Performance of the Device at Different Values of W_{ring}

The device performance at various Wring values is summarized in Table 1. We can observe that by lowering Wring from 800 nm to 500 nm, the sensitivity (S), a Figure of Merit, and Q-factor of the device were improved to 230 nm/RIU, 418.2 RIU-1, and 2247.5, respectively.

Table 1. Ring resonator performance for different values of W_{ring} [10].

W_{ring} (nm)	*S* (nm/RIU)	*FOM* (RIU^{-1})	*Q-Factor*
500	~230	~418.2	2247.5
600	~165	~375	2240
700	~120	~272.7	2227.5
800	~90	~204.5	2239

The findings in this study are incredibly attractive and competitive with those of Si photonics and optical fiber-based sensors. A semiconductor waveguide R.I sensor with S = 235 nm/RIU was tested for a bio-sensing application [42]. According to Carlborg et al., who achieved an experimental sensitivity of 246 nm/RIU with a far more complicated ring resonator layout structure [43], the resulting sensitivity value is similar to silicon nitride slot waveguide ring resonator's sensors.

3.2. Subwavelength Grating Waveguide (SWG Waveguide)

Another investigated structure is an SWG waveguide. It is a structure that may be used to implement a waveguide NIR filter [12, 44-45] or a waveguide Fabry–Pérot (FP)-sensor [12] as shown in Fig. 12 (top) and Fig. 12 (bottom), respectively.

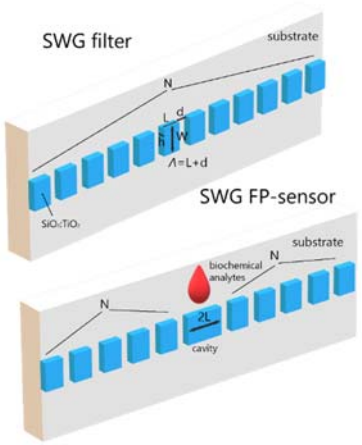

Fig. 12. SWG NIR-filter and FP-sensor structures design [12].

As shown in the schematic representation, an SWG is a structure that relies on many different variables, which if changed affect the response of the whole structure. The main variables of an SWG are W – width of the waveguide, H – the height of the WG, Λ – period of the grating being the sum of L – length of a WG segment, and d – the distance between the segments, N – number of periods. There is also a parameter named *duty cycle* which is the ratio of $\frac{L}{\Lambda}$.

3.2.1. NIR-filter

A NIR-filter is one of the SWG applications. It works based on cutting a certain wavelength window. Light after passing through an SWG in the transmission spectrum is observed as the input spectrum minus a specific range of wavelengths [44]. As a result, SWG WGs can work as bandstop filters. In Fig. 13 the response of the SWG depending on the duty cycle is shown. The change in the duty cycle affects the range of the wavelengths that are blocked by the SWG. The lower the duty cycle, the wider the stopband gets, and the wavelength range shifts towards slightly longer wavelengths.

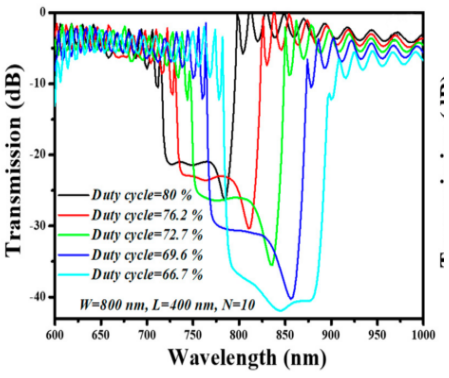

Fig. 13. Transmission spectrum of an SWG NIR filter depending on duty cycle [12].

In Fig. 14 the distribution of the electric field for two different wavelengths is shown, which depicts the operation of an SWG in a very understandable way. For the wavelength in the stopband, the electric field stops propagating through the SWG because of the Bragg reflection [46], and for a wavelength not included in the stopband, the electric field mapping is ordinary.

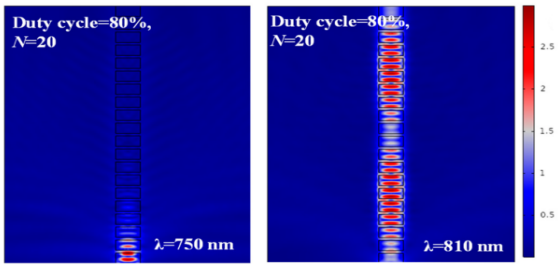

Fig. 14. Electric field mapping in the stopband region (left) and above the stopband region (right) [12].

3.2.2. FP-sensor

A slightly more interesting and more complex photonic structure containing an SWG is an FP-sensor [47]. The sensor is shown in Fig. 12. It is very similar to a regular SWG but instead of being uniform, it has a cavity of 2L size from the waveguide material in the middle of the structure. This results in the formation of a cavity sandwiched between two DBRs. Thus, it creates an FP-sensor. The response of an FP-sensor is shown in Fig. 15.

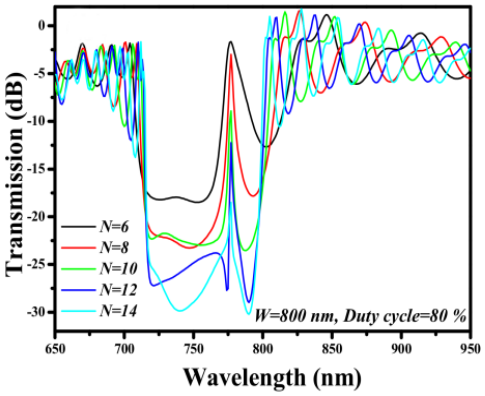

Fig. 15. Transmission spectrum of an SWG FP-sensor [12].

As can be observed, the response also contains a filtered band of light, but it has a specific wavelength within the stopband that is transmitted. It can be called the FP-wavelength. The FP-wavelength changes with the change of the duty cycle as shown in Fig. 16.

It is also affected by the change in the width of the waveguide *W*. The transmission characteristic depending on the change of width is shown in Fig. 17.

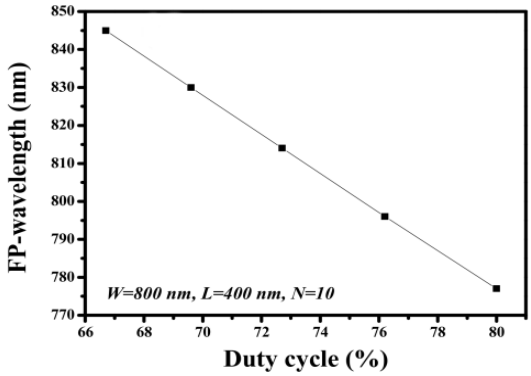

Fig. 16. FP-wavelength on duty cycle dependence [12].

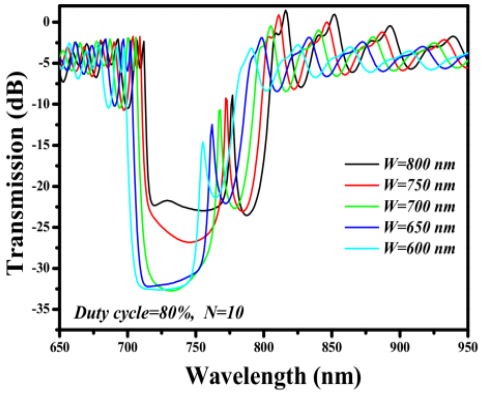

Fig. 17. FP-sensor operation dependance on the width of the waveguide [12].

A shift of the FP-wavelength is observed in the transmitted spectrum. Reading and comparing the shift of the FP-wavelength is the basic principle of operation of an SWG FP-sensor.

By changing the n_{amb} it is also possible to observe the shift of the FP-wavelength. Therefore, by disposing of a biochemical sample on the SWG, the sample can be characterized [48-50].

3.3. 1-D Photonic Crystals

A sensing structure that is somehow similar to an SWG is a 1-D photonic crystal (1-D PhC). The fundamental design structure of a 1-D PhC [51] is shown in Fig. 18. It is a simple waveguide that has a set of identical air holes evenly distributed along the waveguide.

The structure looks similar to an SWG and also has some basic variables that define it, being *a* – lattice constant, *r* – radius of air holes, *W* – width of the waveguide, and *N* – total number of air holes.

This basic 1-D PhC structure performs as a waveguide filter and by changing its variables, for example, the n_{wg}, *r*, or *a*, slight changes in the transmission spectrum are achievable which enables the use of this type of filter for different specific

applications [52]. Some transmission spectra for different variables are shown in Fig. 19. The most important visible effect of the manipulation of n_{wg}, r, or a is the shift of the stopband region. For lower n_{wg} and a the stopband appears for shorter wavelengths. However, for lower r the stopbands shifts towards longer wavelengths.

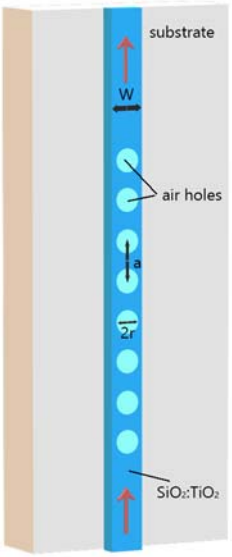

Fig. 18. Schematic 1-D PhC design with basic variables [11].

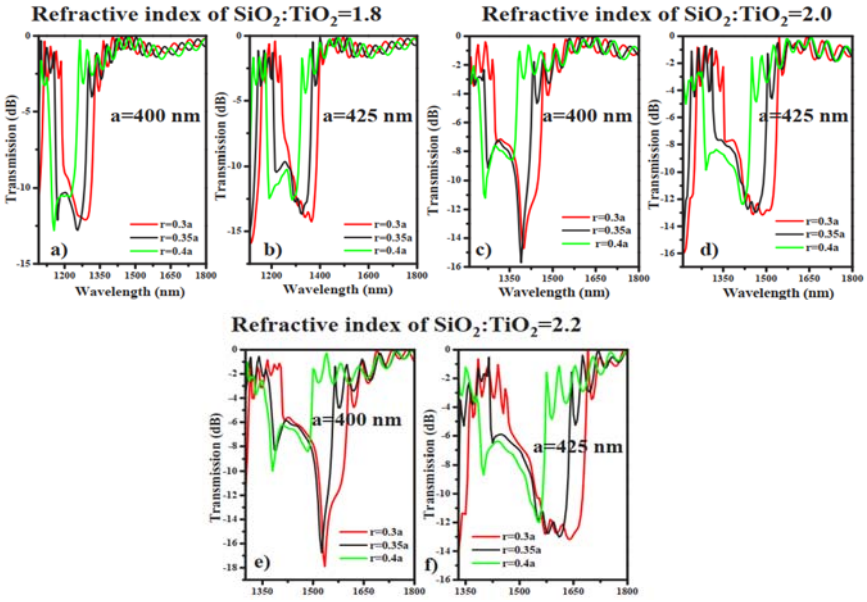

Fig. 19. 1-D PhC filter operation for different variables (a-f) [11].

Another approach to the application of a 1-D PhC would be to design an FP-sensor by adding a cavity in the middle of the periodic structure of the 1-D PhC. The presence of the cavity adds to the transmission spectrum a certain wavelength within the stopband region.

Fig. 20 shows the operation of a 1-D PhC. In a) the schematic diagram of the structure can be observed, showing the cavity and the air holes, b) the transmission spectrum with the visible peak wavelength in the stopband region and c) the Electric field pattern for the resonance peak.

The principle of operation of a 1-D PhC lies in the fact of changing the n_{amb} just as in the SWG FP-sensor. After changing ambient R.I, a shift in the transmission spectrum is visible, therefore the structure can operate as a sensor [53]. An exemplary response is shown in Fig. 21.

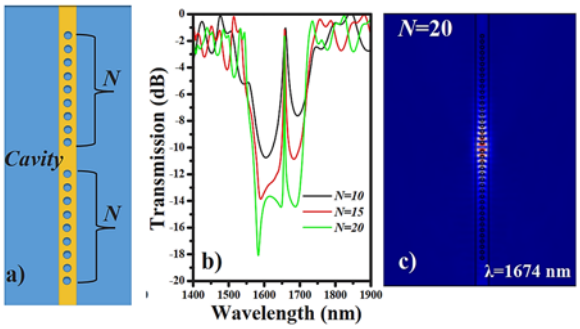

Fig. 20. a) Schematic FP-filter design, b) transmission spectrum, c) Electric field pattern in the resonance peak [11].

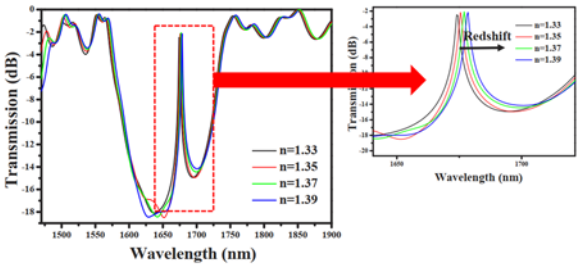

Fig. 21. Sensor operation of a 1-D PhC depending on the change of n_{amb} [11].

The sensitivity of the device can be easily calculated by the formula (1) previously mentioned.

The sensitivity of the device is also affected by the width of the waveguide as in Table 2. The device becomes more sensitive if narrower waveguides are used.

Table 2. Sensitivity dependence of the structure on waveguide width [11].

W (nm)	*N*	*a* (nm)	*r*	*S* (nm/RIU)
1000	20	425	0.3a	75
800	20	425	0.3a	100-108
600	20	425	0.3a	175

4. Conclusions

The numerical analyses and performances of different devices such as ring resonators, subwavelength grating, and photonic crystal waveguides show promising results and the SiO_2:TiO_2 platform can be utilized in several applications due to its exceptional physical, chemical, and optical properties. This platform has great potential when paired with nano-imprint lithography for the fabrication of integrated photonic devices in a single step. We believe that the studies presented in this mini-review will be useful for the researchers working on the topic of silica-titania sol-gel deposited via the dip-coating method and the realization of photonic devices based on this interesting platform.

Acknowledgements

This work was funded with the project "Hybrid sensor platforms of integrated photonic systems based on ceramic and polymer materials" carried out within the TEAM-NET program of the Foundation for Polish Science financed by the European Union under the European Regional Development Fund, POIR.04.04.00-00-14D6/18.

References

[1]. M. A. Butt, S. N. Khonina, N. L. Kazanskiy. Optical elements silicon photonics, *Comput. Opt.,* 43, 2019, pp. 1079–1083.

[2]. M. A. Butt, N. L. Kazanskiy, Two-dimensional photonic crystal heterostructure for light steering and TM-polarization maintaining applications, *Laser Phys.*, 31, 2021, 036201.

[3]. D. X. Dai, S. P. Wang, Asymmetric directional couplers based on silicon nanophotonic waveguides and applications, *Front. Optoelectron*, 9, 2016, pp. 450–465.

[4]. L. Dan, D. S. Citrin, S. Hu, Compact high-performance polarization beam splitter based on a silicon photonic crystal heterojunction, *Opt. Mater.,* 109, 2020, 110256.

[5]. G. R. Chen, J. W. Choi, E. Sahin, D. T. Ng, D. H. Tan, On-chip 1 by 8 coarse wavelength division multiplexer and multi-wavelength source on ultra-silicon-rich nitride, *Opt. Express*, 27, 2019, pp. 23549–23557.

[6]. M. A. Butt, A. Kaźmierczak, C. Tyszkiewicz, P. Karasinski, R. Piramidowicz, Recent Advances in the Realization of a Low-Cost Integrated Photonic Platform Developed via a Sol-Gel Dip-Coating Method, in *Proceedings of the 8th International conference on Sensors and Electronics Instrumentation Advances (SEIA'2022)*, 21-23 September 2022, Greece, 2022, pp. 45-47.

[7]. P. Karasinski, C. Tyszkiewicz, R. Piramidowicz, and A. Kazmierczak, Development of integrated photonics based on SiO_2:TiO_2 sol-gel derived waveguide layers: state of the art, perspectives, prospective applications, *Proc. SPIE*, 11364, 2020, 1136414.

[8]. P. Karasinski, C. Tyszkiewicz, A. Domanowska, A. Michalewicz, and J. Mazur, Low loss, long time stable sol-gel derived silica-titania waveguide films, *Mater. Lett.,* 143, 2015, pp. 5–7.

[9]. A. Lukowiak, R. Dylewicz, S. Patela, W. Strek, and K. Maruszewski, Optical properties of SiO_2-TiO_2 thin film waveguides obtained by the sol-gel method and their applications for sensing purposes, *Opt. Mater.*, 27, 9, 2005, pp. 1501–1505.

[10]. Butt, M. A., Kazmierczak, A., Tyszkiewicz, C., Karasinski, P., Piramidowicz, R. Mode Sensitivity Exploration of Silica–Titania Waveguide for Refractive Index Sensing Applications, *Sensors*, 21, 2021, 7452.

[11]. Butt, M. A., Tyszkiewicz, C., Karasiński, P., Zięba, M., Hlushchenko, D., Baraniecki, T., Kaźmierczak, A., Piramidowicz, R., Guzik, M. and Bachmatiuk, A.,

Development of a low-cost silica-titania optical platform for integrated photonics applications, *Optics Express,* 30, 13, 2022, pp. 23678-23694.

[12]. Butt, M. A., Tyszkiewicz, C., Wojtasik, K., Karasinski, P., Ka ´zmierczak, A., Piramidowicz, R. Subwavelength Grating Waveguide Structures Proposed on the Low-Cost Silica–Titania Platform for Optical Filtering and Refractive Index Sensing Applications, *Int. J. Mol. Sci.*, 23, 2022, 6614.

[13]. Karasinski, P., Jaglarz, J., Mazur, J., Low loss silica-titania waveguide films, *Photonics Lett. Pol.,* Vol. 2, No. 1, 2010, pp. 37-39.

[14]. Kazmierczak, A., Slowikowski, M., Pavlov, K., Filipiak, M., Vervaeke, M., Tyszkiewicz, C., Ottevaere, H., Piramidowicz, R., Karasinski, P. Efficient, low-cost optical coupling mechanism for TiO_2-SiO_2 sol-gel derived slab waveguide surface grating coupler sensors, *Opt. Appl.* 4, 2020, pp. 539–549.

[15]. Innocenzi, P., Martucci, A., Guglielmi, M., Armelao, L., Pelli, S., Righini, G., Battaglin, G. Optical and surface properties of inorganic and hybrid organic–inorganic silica–titania sol–gel planar waveguides, *J. Non-Cryst. Solids,* 259, 1999, pp. 182–190.

[16]. Karasinski, P., Tyszkiewicz, C., Piramidowicz, R., Kazmierczak, A., Development of integrated photonics based on SiO_2:TiO_2 sol-gel derived waveguide layers:state of the art, perspectives, prospective applications, *Proceedings of the SPIE 11364, Integrated Photonics Platforms: Fundamental Research, Manufacturing and Applications, SPIE Photonics Europe,* Strasbourg, France, 29 March–2 April 2020, 1136414.

[17]. Dezfuli, S. M., Sabzi, M. Deposition of self-healing thin films by the sol–gel method: A review of layer-deposition mechanisms and activation of self-healing mechanisms, *Appl. Phys*. *A*, 125, 2019, p. 557.

[18]. Inoue, H., Iwamoto, T., Horie, K., Makishima, A., Ikemoto, M. Preparation and properties of sol-gel thin films with porphins, *J. Opt. Soc. Am.,* B, 9, 1992, pp. 816–818.

[19]. M. Butt, E. S. Kozlova, S. N. Khonina, and R. V. Skidanov, Optical planar waveguide sensor based on (Yb,Nb): RTP/RTP(001) system for the estimation of metal coated cells, *CEUR Workshop Proc.,* 1638, 2016, pp. 16–23.

[20]. X. Orignac, D. Barbier, X. M. Du, R. M. Almeida, O. McCarthy, and E. Yeatman, Sol-gel silica/titania-on-silicon Er/Yb-doped waveguides for optical amplification at 1.5 μm, *Opt. Mater.,* 12, 1, 1999, pp. 1–18.

[21]. A. I. Gomez-Varela, Y. Castro, A. Duran, P. A. Beule, M. T. Flores-Arias, and C. Bao-Varela, Synthesis and characterization of erbium-doped SiO_2-TiO_2 thin films prepared by sol-gel and dip-coating techniques onto commercial glass substrates as a route for obtaining active Gradient-index materials, *Thin Solid Films,* 583, 2015, pp. 115–121.

[22]. Y. Sorek, R. Reisfeld, and A. M. Weiss, Effect of composition and morphology on the spectral properties and stability of dyes doped in a sol-gel glass waveguide, *Chem. Phys. Lett.*, 244, 5-6, 1995, pp. 371–378.

[23]. A. Yimit, K. Itoh, and M. Murabayashi, Detection of ammonia in the ppt range based on a composite optical waveguide pH sensor, *Sens. Actuators, B,* 88, 3, 2003, pp. 239–245.

[24]. A. D'Orazio, M. D. Sario, L. Mescia, V. Petruzzelli, and F. Prudenzano, Design of Er3+Yb3+ doped silica/titania planar waveguide amplifier, in *Proceedings of 2003 5th International Conference on Transparent Optical Networks*, Warsaw, Poland, 2003.

[25]. P. Karasinski, Sol-gel derived optical waveguide films for planar sensors with phase modulation, *Opt. Appl.*, 34, 4, 2004, pp. 467–475.

[26]. Karasinski, P., Tyszkiewicz, C., Rogozinski, R., Jaglarz, J., Mazur, J. Optical rib waveguides based on sol-gel derived silica-titania films, *Thin. Solid Films,* 519, 2011, pp. 5544–5551.

[27]. Khlyustova, A., Cheng, Y., Yang, R. Vapor-deposited functional polymer thin films in biological applications, *J. Mater. Chem. B*, 8, 2020, pp. 6588–6609.

[28]. Royer, F., Jamon, D., Rousseau, J. J., Roux, H., Zins, D., Cabuil, V. Magneto-optical nanoparticle-doped silica-titania planar waveguides, *Appl. Phys. Lett.,* 86, 2005, 011107.

[29]. Roy, R. D., Sil, D., Jana, S., Biswas, P. K., Bhadra, S. K., Experimental study of perfectly patterned silica-titania optical waveguide, *Photonic Sensors*, 2, 2012, pp. 81–91.

[30]. Almeida, R., Marques, A., Pelli, S., Righini, G., Chiasera, A., Mattarelli, M., Spectroscopic assessment of silica-titania and silica-hafnia planar waveguides, *Philos. Mag.,* 84, 2006, pp. 1659–1666.

[31]. G. Brusatin, M. Guglielmi, P. Innocenzi, A. Martucci, G. Battaglin, S. Pelli, G. Righini, Microstructural and optical properties of sol-gel silica-titania waveguides, *Journal of Non-Crystalline Solids*, Vol. 220, Issues 2–3, 1997, pp. 202-209.

[32]. Leszek Golonka, Pawel Bembnowicz, Dominik Jurków, Karol Malecha, Henryk Roguszczak, Rafał Tadaszak, Ceramic Microsystems, in *Proceedings of the International Microelectronics Assembly and Packaging Society Conference,* Poland Chapter, 2010.

[33]. Giancarlo Righini, Stefano Pelli, Sol-Gel Glass Waveguides. *Journal of Sol-Gel Science and Technology*, 8. 1997, pp. 991-997.

[34]. Vasconcelos, Helena, Optical Waveguides Based on Sol-Gel Coatings, in Electromagnetic Propagation and Waveguides in Photonics and Microwave Engineering (Patrick Steglich, Ed.), *Intechopen*, 2020.

[35]. Rafał Tadaszak, Anna Lukowiak, Leszek Golonka, Sergiusz Patela, Hybrid sol-gel-glaze planar optical waveguides on LTCC substrate - Preliminary works, *Optica Applicata*, 41, 2011.

[36]. K. Nowak et al., Sol-gel-based optical waveguides on LTCC substrates, in *Proceedings of the 31st International Spring Seminar on Electronics Technology,* 2008, pp. 518-522.

[37]. Muhammad A. Butt, Thin-Film Coating Methods: A Successful Marriage of High-Quality and Cost-Effectiveness - A Brief Exploration, *Coatings*, 12, 2022, 1115.

[38]. N. Golshani et al., Low-loss, low-temperature PVD SiN waveguides, in *Proceedings of the 17th IEEE International Conference on Group IV Photonics (GFP),* 2021, pp. 1-2.

[39]. Mark P. Hiscocks, Christopher J. Kaalund, François Ladouceur, Shane T. Huntington, Brant C. Gibson, Steven Trpkovski, David Simpson, Eric Ampem-Lassen, Steven Prawer, James E. Butler, Reactive ion etching of waveguide structures in diamond, *Diamond and Related Materials,* Vol. 17, Issue 11, 2008, pp. 1831-1834.

[40]. Axel Grosse et al, Deep wet etching of fused silica glass for hollow capillary optical leaky waveguides in

microfluidic devices, *J. Micromech. Microeng*, 11, 2001, 257.
[41]. Nikolay L. Kazanskiy, Svetlana N. Khonina, Muhammad A. Butt, Advancement in Silicon Integrated Photonics Technologies for Sensing Applications in Near-Infrared and Mid-Infrared Region: A Review, *Photonics,* 9, 2022, 331.
[42]. Wang, Y., Gao, B., Zhang, K., Yuan, K., Wan, Y., Xie, Z., Xu, X., Zhang, H., Song, Q., Yao, L., et al. Refractive Index Sensor Based on Leaky Resonant Scattering of Single Semiconductor Nanowire, *ACS Photon.*, 4, 2017, pp. 688–694.
[43]. Carlborg, C. F., Gylfason, K. B., Kaźmierczak, A., Dortu, F., Polo, M. J. B., Catala, A. M., Kresbach, G., Sohlström, H., Moh, T., Vivien, L., et al., A packaged optical slot-waveguide ring resonator sensor array for multiplex label-free assays in labs-on-chips, *Lab Chip,* 10, 2010, pp. 281–290.
[44]. Junjia Wang, Ivan Glesk, and Lawrence R. Chen, Subwavelength grating filtering devices, *Opt. Express*, 22, 2014, pp. 15335-15345.
[45]. Wang, J., Glesk, I. and Chen, L., Subwavelength grating Bragg grating filters in silicon-on-insulator, *Electron. Lett.,* 51, 2015, pp. 712-714.
[46]. Junjia Wang, Ivan Glesk, Lawrence R. Chen, Subwavelength grating devices in silicon photonics, *Science Bulletin*, Vol. 61, Issue 11, 2016, pp. 879-888.
[47]. N. L. Kazanskiy; M. A. Butt; S. N. Khonina, Silicon photonic devices realized on refractive index engineered subwavelength grating waveguides-A review, *Optics & Laser Technology*, 138, 2021, 106863.
[48]. N. Kazanskiy, S. Khonina, M. Butt, A. Kaźmierczak, R. Piramidowicz, State-of-the-Art Optical Devices for Biomedical Sensing Applications—A Review, *Electronics,* 10, 2021, 973.
[49]. M. A. Butt, S. N. Khonina & N. L. Kazanskiy, Numerical analysis of a miniaturized design of a Fabry–Perot resonator based on silicon strip and slot waveguides for bio-sensing applications, *Journal of Modern Optics,* 66, 11, 2019, pp. 1172-1178.
[50]. Wei Liang, Yanyi Huang, Yong Xu, Reginald K. Lee, and Amnon Yariv, Highly sensitive fiber Bragg grating refractive index sensors, *Appl. Phys. Lett.*, 86, 2005, 151122.
[51]. Nikolai Lvovich Kazanskiy, Muhammad Ali Butt, One-dimensional photonic crystal waveguide based on SOI platform for transverse magnetic polarization-maintaining devices, *Phot. Lett. Pol.,* Vol. 12, No. 3, 2020, pp. 85-87.
[52]. M. A. Butt, S. N. Khonina, N. L. Kazanskiy, Recent advances in photonic crystal optical devices: A review, *Optics & Laser Technology*, 142, 2021, 107265.
[53]. Muhammad A. Butt, Nikolay L. Kazanskiy, Svetlana N. Khonina, Advances in Waveguide Bragg Grating Structures, Platforms, and Applications: An Up-to-Date Appraisal, *Biosensors,* 12, 2022, 497.